

The effect of massive binaries on stellar populations and supernova progenitors

John J. Eldridge,^{1,2★} Robert G. Izzard³ and Christopher A. Tout²

¹*Astrophysics Research Centre, Physics Building, Queen's University, Belfast, County Antrim BT7 1NN*

²*Institute of Astronomy, The Observatories, University of Cambridge, Madingley Road, Cambridge CB3 0HA*

³*Sterrekundig Instituut Utrecht, Postbus 80000, 3508 TA Utrecht, the Netherlands*

Accepted 2007 November 19. Received 2007 November 8; in original form 2007 September 25

ABSTRACT

We compare our latest single and binary stellar model results from the Cambridge STARS code to several sets of observations. We examine four stellar population ratios: the number of blue to red supergiants, the number of Wolf–Rayet stars to O supergiants, the number of red supergiants to Wolf–Rayet stars and the relative number of Wolf–Rayet subtypes, WC to WN stars. These four ratios provide a quantitative measure of nuclear burning lifetimes and the importance of mass loss during various stages of the stars' lifetimes. In addition, we compare our models to the relative rate of Type Ib/c to Type II supernovae to measure the amount of mass lost over the entire lives of all stars. We find reasonable agreement between the observationally inferred values and our predicted values by mixing single and binary star populations. However, there is evidence that extra mass loss is required to improve the agreement further, to reduce the number of red supergiants and increase the number of Wolf–Rayet stars.

Key words: binaries: general – stars: evolution – supergiants – supernovae: general – stars: Wolf–Rayet.

1 INTRODUCTION

There are many problems outstanding in the field of stellar evolution. As regards the most-massive stars, those that end their lives as a supernova (SN), the main questions are ‘at what rate do stars lose mass?’, ‘which stars give rise to which SNe?’, ‘what physical processes occur in binary systems?’ and ‘how important are rotation and magnetic fields?’ One way to gain insight into these questions is to observe populations of stars and SNe. Massive stars are classified in a range of possible spectroscopic stellar types. The main categories are blue supergiants (BSGs), red supergiants (RSGs) and Wolf–Rayet (WR) stars. If we count the numbers of such stars in a single system (e.g. a stellar cluster or galaxy), we can test the accuracy of our stellar models by comparing to model predictions.

When such comparisons are performed, the agreement can be poor. For example, the ratio of the BSG to RSG populations has been an outstanding problem for some time (Langer & Maeder 1995; Maeder & Meynet 2001; Massey & Olsen 2003). The ratio of the number of RSGs to the number of WR stars is also not correctly predicted by stellar models (Massey 2003). However, the ratios of WR star subtypes, WN to WC stars, are predicted by modern stellar evolution (Meynet & Maeder 2005; Eldridge & Vink 2006).

Massive single stars end their lives as core-collapse SNe but the relation between the star and SN type is not straightforward. A list

of core-collapse SN types includes Types IIP, IIL, IIB, IIn, IIpec, Ib and Ic¹ (Turatto, Benetti & Pastorello 2007). The difference between Type II and Type I SNe is the presence or absence of hydrogen in the SN spectrum. It is easy to identify which stellar models contain hydrogen or not but the subtype classifications are fairly arbitrary (Popov 1993; Dray & Tout 2003; Heger et al. 2003; Eldridge & Tout 2004b; Young, Smith & Johnson 2005). The most-direct method to link SNe to stellar end-point models is to search for the progenitor stars of SNe in pre-explosion images (Van Dyk, Li & Filippenko 2003; Smartt et al. 2004).

If we only split the SN types into Type II and Type Ib/c, another comparison can be made between models and observations. The relative rates of these two SN types and how they vary with metallicity have been estimated observationally (Prantzos & Boissier 2003). Meynet & Maeder (2005) have shown that standard non-rotating single-star models do not agree with these observed rates and that mass loss must be enhanced, in their case by rotation, to find an agreement between predicted SN ratios and those inferred from observations.

The studies mentioned so far only compare single-star models to the observations. This ignores the observed fact that many stars are in binaries. Binary evolution has been studied widely (e.g.

¹ Type Ia SNe are thought to be thermonuclear events from explosive carbon burning in a degenerate carbon–oxygen white dwarf and are not considered in this work.

★E-mail: jje@ast.cam.ac.uk

Podsiadlowski, Joss & Hsu 1992; Wellstein & Langer 1999; Belczynski, Kalogera & Bulik 2002; Izzard, Ramirez-Ruiz & Tout 2004; Dray & Tout 2007; Vanbeveren, Van Bever & Belkus 2007; Vázquez et al. 2007). The methods employed to estimate the effect of binaries are based either on rapid population synthesis or on a small number of detailed models. Population synthesis employs formulae or tables based on detailed models to follow the evolution, (e.g. Hurley, Pols & Tout 2000 and the evolution of a star can be calculated in a fraction of a second rather than many minutes taken by a detailed code. The speed of calculations means that the full range of parameters that govern the outcome of binary evolution can be studied and their relative effects evaluated. The disadvantage is that in the complex phases of evolution, such as when the envelope is close to being stripped, the results of population synthesis can be quite spurious.

We have constructed a set of binary stellar models covering a wide range of binary parameter space using a detailed stellar evolution code (Eldridge & Tout 2004a). With these models, we have investigated the effect binary evolution has on the lifetimes of the various phases of stellar evolution and therefore the effect it has on the relative populations of massive stars and the relative numbers of different types of SNe. While the binary parameter-space resolution is low compared to rapid population-synthesis studies, it is still one of the highest-resolution studies undertaken with a detailed evolution code.

We note that we do not consider here the effect of rotation or magnetic fields. The effect of rotation on the structure and evolution of stars is a complicated process and has been studied by Heger, Langer & Woosley (2000) and Heger & Langer (2000) and the extensive study beginning with Meynet & Maeder (1997) and continuing up to most recently in Meynet & Maeder (2007). The effect of magnetic fields on stellar structure and evolution has also been investigated by Meynet & Maeder (2003), Meynet & Maeder (2004) and Heger, Woosley & Spruit (2005). Our code does not include rotation; therefore, our study reveals the importance of duplicity alone. We discuss how rotation may affect our results in Section 6.

In this paper, we start by providing details of our stellar model construction. We then specify our definitions of the different phases of stellar evolution and discuss how binary evolution affects the relative lifetimes of stars in various phases of stellar evolution. Using these lifetimes we predict how the BSG to RSG, the WR to O supergiant, the RSG-to-WR and WC-to-WN ratios vary with metallicity. We then predict how the relative rates of Type Ib/c and Type II SNe vary with metallicity. With each of these predictions, we compare the values to the ratios inferred from observations. Finally, we discuss the implications of our results.

2 CONSTRUCTION AND TESTING OF THE STELLAR MODELS

We use a detailed stellar evolution code to construct sets of single and binary star models rather than a rapid population-synthesis code, because we require accurate treatment of complex stages of evolution, such as when the envelope is close to being stripped, to obtain more accurate pre-SN models. We model the binary parameters with a reasonable resolution owing to the great amount of computer power that is now available. We have compared our binary models to the predictions of a rapid population-synthesis code (Izzard & Tout 2003; Izzard et al. 2004, 2006) and found reasonable agreement for most of our predictions. However, difficulty in assigning WR types to population-synthesis helium stars meant that the agreement was poor for the WC/WN ratio.

2.1 Detailed single-star models

Our detailed stellar models were calculated with the Cambridge stellar evolution code, STARS, originally developed by Eggleton (1971) and updated most recently by Pols et al. (1995) and Eldridge & Tout (2004a). Further details can be found at the code's web pages.² Our models are available from the same location for download without restriction. They are similar to those described by Eldridge & Tout (2004b) but we use 46 rather than 21 zero-age main-sequence models. Every integer mass from 5 to 40 M_{\odot} is modelled along with 45, 50, 55, 60, 70, 80, 100 and 120 M_{\odot} . The initially uniform composition is $X = 0.75 - 2.5Z$ and $Y = 0.25 + 1.5Z$, where X is the mass fraction of hydrogen, Y that of helium and Z is the initial metallicity taking the values 0.001, 0.004, 0.008, 0.02 and 0.04. The composition mixture is scaled solar and $Z_{\odot} = 0.02$. Our models end after core carbon-burning or at the onset of core neon-ignition. During these burning stages, the envelope is only affected to a small degree because $t_{\text{nuclear}} \ll t_{\text{thermal}}$. Furthermore, the late stages of evolution are rapid and have a negligible effect on the final observable state of the progenitor (Woosley, Heger & Weaver 2002).

Our opacity tables include the latest low-temperature molecular opacities of Ferguson et al. (2005). This update leads to tiny changes in the radii and surface temperatures of RSG models because the altered opacity values only slightly modify the surface boundary conditions.

All the models employ our standard mass-loss prescription because it agrees best with observations of SN progenitors (Eldridge & Tout 2004b). The prescription is based on that of Dray & Tout (2003) but modified in several ways. For pre-WR mass loss, we use the rates of de Jager, Nieuwenhuijzen & van der Hucht (1988) except for OB stars for which we use the theoretical rates of Vink, de Koter & Lamers (2001). When the star becomes a WR star [$X_{\text{surface}} < 0.4$, $\log(T_{\text{eff}}/K) > 4.0$], we use the rates of Nugis & Lamers (2000). We scale all rates with the standard factor $(Z/Z_{\odot})^{0.5}$ (Kudritzki, Pauldrach & Puls 1987; Heger et al. 2003), except for the rates of Vink et al. (2001) which include their own metallicity scaling.

The most-important change is that we scale the WR mass-loss rates with the metallicity, even though this is not normally included. Vanbeveren (2001) first included the scaling in a population-synthesis model while Crowther et al. (2002) first suggested that the scaling should be included from observations of WR stars in the Large Magellanic Cloud (LMC) and in the Galaxy. Recent theoretical predictions also suggest that the scaling should be included (Vink & de Koter 2005). Inclusion of this scaling results in a greater agreement with the change in WR population ratios with metallicity (Eldridge & Vink 2006). There is some uncertainty in the exact magnitude of the exponent we should use. To remain consistent, we use the same exponent as for the non-WR stars.

We synthesize a single-star population by assuming a constant star formation rate and the initial mass function (IMF) of Kroupa, Tout & Gilmore (1993).

2.2 Detailed binary models

Binary stars experience different evolution from that of single stars if their components interact. In a wide-enough orbit, a star is not affected by a companion. Duplicity allows the possibility of enhanced mass loss, mass transfer and other binary specific interactions (e.g. irradiation, colliding winds, surface contact, gravitational

² <http://www.ast.cam.ac.uk/~stars>

distortion) and hence a greater scope for interesting evolutionary scenarios.

We have modified our stellar evolution code to model binary evolution. The details of our binary interaction algorithm are relatively simple compared to the scheme outlined in Hurley, Tout & Pols (2002). We use their scheme as a basis but we change some details which cannot be directly applied to our detailed stellar evolution calculation. We also make a number of assumptions in producing our code to keep it relatively simple. Our aim is to investigate the effect of enhanced mass loss due to binary interactions on stellar lifetimes and populations; therefore, we concentrate on this rather than every possible physical process which would add more uncertainty to our model. We also make assumptions in calculating our synthetic population to avoid calculating a large number of models. For example, we do not model the accretion on to the secondary in the detailed code. We take the final mass of the secondary at the end of the primary code as the initial mass of the secondary when we create our detailed secondary model. This avoids calculating 10 times more secondary models than primary models.

2.2.1 Evolution of a binary

In our binary models, we always treat the primary as the initially more massive star and we only evolve one star at a time with our detailed code. When we evolve the primary in detail, it has a shorter evolutionary time-scale than the secondary which remains on the main sequence until after the primary completes its evolution and so we can determine the state of the secondary using the single stellar evolution equations of Hurley et al. (2000). When we evolve the secondary in detail, we assume that its companion is the compact remnant of the primary (a white dwarf, neutron star or black hole) and treat this as a point mass. We describe how we combine these models to synthesize a population below.

To model a binary, we begin by specifying a primary mass, M_1 , a secondary mass, M_2 , and an initial separation, a . We assume that the orbit is circular and conserve angular momentum unless mass is lost from the system. We follow the rotation of the stars, considering them to rotate as solid bodies but we do not include processes such as rotationally enhanced mass loss or mixing. We give the stars initial rotation rates linked to their initial masses as in Hurley et al. (2000). When the stars lose mass in their stellar wind angular momentum is lost both from their spin and from their orbit. We ignore tides so stellar rotation and orbital rotation evolve independently until Roche lobe overflow (RLOF) when we force the stars into synchronous rotation with the orbit, transferring angular momentum from the spin to the orbit or vice versa.

2.2.2 Roche lobe overflow

In a binary system, the equipotential surfaces are not spherical but are distorted by the gravity of the companion star and by the rotation of the system. If the stars are small compared to the size of the orbital separation, these surfaces are nearly spherical but as the star grows relative to the separation the shape is distorted and becomes more ellipsoidal. A star's surface eventually reaches the L1 Lagrange point where the gravity of both stars cancels exactly. If a star expands beyond this point, then material begins to flow towards the other star. To include this in our models, we define a Roche lobe radius, R_{L1} , such that the sphere of this radius has the same volume as the material within the Roche lobe defined by the equipotential surface passing through the L1 point. Therefore, when the star has a radius

greater than the Roche lobe radius it transfers material on to the other star. We use the Roche lobe radius given by Eggleton (1983):

$$\frac{R_{L1}}{a} = \frac{0.49q_1^{2/3}}{0.6q_1^{2/3} + \ln(1 + q_1^{1/3})}, \quad (1)$$

where $q_1 = M_1/M_2$ and a is the orbital separation. It is accurate to within 2 per cent for the range $0 < q_1 < \infty$. When $R_1 > R_{L1}$, we calculate the rate at which mass is lost from the primary according to

$$\dot{M}_{IR} = F(M_1) \left[\ln \left(\frac{R_1}{R_{L1}} \right) \right]^3 M_{\odot} \text{ yr}^{-1}, \quad (2)$$

where

$$F(M_1) = 3 \times 10^{-6} [\min(M_1, 5.0)]^2, \quad (3)$$

chosen by experiment to ensure that mass transfer is steady (Hurley et al. 2002).

Mass lost from the primary is transferred to the secondary but not all is necessarily accreted. Accretion causes the star to expand owing to increased total mass and therefore an increased energy-production rate if $\dot{M}_2 \geq M_2/\tau_{KH}$, where τ_{KH} is the thermal, or Kelvin–Helmholtz, time-scale. We assume that the star's maximum accretion rate is determined by its current mass and its thermal time-scale. We define a maximum accretion rate for a star such that $\dot{M}_2 \leq M_2/\tau_{KH}$. If the accretion rate is greater than this, then any additional mass and its orbital angular momentum are lost from the system. In general, stars with lower masses have longer thermal time-scales than more massive stars. Efficient transfer is only possible if the two stars are of nearly equal mass so the thermal time-scales are similar. This is an approximate treatment but provides a similar result to the more complex model of Petrovic, Langer & van der Hucht (2005b) who included rotation and found that it led to inefficient mass transfer. For compact companions, we derive the maximum accretion rate from the Eddington limit (Cameron & Mock 1967).

2.2.3 Common-envelope evolution

If RLOF occurs but does not arrest the expansion of the mass-losing star, growth continues until the secondary is engulfed in the envelope of the primary. This is common-envelope evolution (CEE). During CEE it is thought that the envelope is ejected by some dynamical process and that the principal source of energy for the envelope ejection is the orbital energy (Paczynski 1976; Livio & Soker 1984). The orbital separation decreases and there is a chance that the two stars may coalesce before the envelope is ejected. Alternatively, the two stars are left in a close orbit, commonly one helium star for a massive progenitor and one main-sequence star. If the secondary then evolves to a helium giant, a second CEE phase can occur possibly leading to a merger or a very close binary.

CEE is modelled in population synthesis by first calculating the energy required for the ejection of the envelope, the binding energy, $E_{1, \text{bind}} = GM_1 M_{1, \text{env}} / (\lambda R_1)$, where $M_{1, \text{env}}$ is the mass of the envelope, R_1 is the radius of the star and λ is a constant to reflect the structure of the envelope. This is then compared to the initial orbital energy, $E_{\text{orb}, i} = -GM_{c,1} M_2 / (2a_i)$, where $M_{c,1}$ is the mass of the core and a_i is the initial separation at the onset of CEE. If there is not enough orbital energy to eject the envelope and leave a stable binary, then the two stars merge to form one star. Otherwise the envelope is removed leaving a stable binary system (e.g. Hurley et al. 2002). The new orbit is calculated by the equation $E_{1, \text{bind}} = \alpha_{\text{CE}} (E_{\text{orb}, i} - E_{\text{orb}, f})$, where $E_{\text{orb}, f}$ is the final orbital energy from which the final

separation is calculated. There is some uncertainty in the constant α_{CE} as there are other sources of energy available such as the energy from nuclear reactions and re-ionization energy of the hydrogen in the envelope so it can be greater than 1.

In our models when CEE occurs, we derive the mass-loss rate from the above equation for RLOF; however, we limit the mass-loss rates to a maximum of $10^{-3} M_{\odot} \text{ yr}^{-1}$ because more rapid mass loss causes the evolution code to break down. We assume that the secondary accretes no mass because the CEE occurs on the thermal time-scale of the primary which is normally shorter than the thermal time-scale of the less-massive secondary. The accretion rate for a compact remnant is restricted to the Eddington limit (Cameron & Mock 1967). To calculate the change in the orbital separation, we calculate the binding energy of the material lost in the CEE wind ($\delta E_{\text{binding}} = -(M_1 + M_2) \delta M_1 / R_1$) and remove it from the orbital energy [$E_{\text{orbit}} = -GM_1 M_2 / (2a)$]. We find

$$\delta a = \frac{a^2}{R_1} \frac{M_1 + M_2}{M_2} \frac{\delta M_1}{M_1}, \quad (4)$$

where δa is the change in orbital separation and δM_1 is the mass lost in the time-period considered, one model time-step. In this formalism, δM_1 is negative so the orbit shrinks. By determining the mass-loss rate from the RLOF equation, we find that the CEE ends naturally with the stellar radius shrinking once most of the envelope has been removed.

2.2.4 Binary mergers

In the most-compact binaries, the stars can merge during CEE to form a single star whose mass is the sum of its parents. We find that some of our binary models enter CEE and the binary separation tends to zero. When this occurs we use a different binary model. The primary is evolved in the detailed code and once its radius is equal to the binary separation all the mass of the secondary is accreted on to the surface of the primary star and the evolution continues as a more massive single star. This is an extremely simple model. Other models such as Podsiadlowski et al. (1992) show that a more detailed treatment may be required but the efficiency of the merger is always uncertain. Our models provide an estimate of the effects of stellar mergers and are an upper limit as we assume that all the secondaries' mass is accreted. Further to the fact that the outcome depends on the evolutionary state of the primary, it is possible that fresh hydrogen could be mixed into the helium-burning zone and therefore cause the envelope to be explosively removed (Podsiadlowski, Morris & Ivanova 2006).

2.2.5 The binary model subsets

We calculate three subsets of binary models which we then combine to simulate a population of stars. The first subset consists of our primary models where we evolve the primary star in the detailed code and evolve the secondary according to the single-star evolution equation of Hurley et al. (2000). We choose our grid to be $M_1 = 5, 6, 7, 8, 9, 10, 11, 12, 13, 15, 20, 25, 30, 40, 60, 80, 100$ and 120 ; $q = M_2/M_1 = 0.1, 0.3, 0.5, 0.7$ and 0.9 ; $\log(a/R_{\odot}) = 1.0, 1.25, 1.5, 1.75, 2, 2.25, 2.5, 2.75, 3, 3.25, 3.5, 3.75$ and 4 . We do not model lower masses because these stars are never luminous enough to affect our population ratios and do not lead to core-collapse SNe.

The second subset consists of our secondary models where we evolve the secondary in the detailed code after the end of the primary evolution and replace the primary by its remnant. We chose three masses for the compact companion to model a white dwarf, neutron

star or black hole, $M_{1,\text{post-SN}} = 0.6, 1.4$ or $2 M_{\odot}$, respectively. We choose the grid to use the same separation and mass grid as for our primary model subset. The final subset consists of our merger models and we choose this grid to have the same M_1, a and q distribution as our primary model. We only calculate models with initial orbital separation smaller than the maximum stellar radius for each initial primary mass. These are only used if the orbital separation reaches zero in a primary model.

2.2.6 Synthesizing the population

The binary population is synthesized by first assuming that the primary masses are distributed with the IMF of Kroupa et al. (1993). We then assume flat distribution over $1 \leq \log(a/R_{\odot}) \leq 4$ and $0.1 \leq q \leq 0.9$. We calculate the primary stars' lifetimes and SN types using the primary models. If a primary model during evolution enters a CEE and the binary separation shrinks to zero, we replace the primary model with a merger model.

The end-point of the primary model is taken to be at the onset of neon-burning, or the onset of thermal pulses in an asymptotic giant branch (AGB) star. First, we determine the remnant the primary will form. A white dwarf is selected unless the primary underwent an SN if there is an oxygen–neon core and the carbon–oxygen core mass is greater than $1.3 M_{\odot}$ when a neutron star is selected. A black hole remnant replaces this if the helium core mass is greater than $8 M_{\odot}$. In the case of a white dwarf, the system remains bound. When a neutron star is formed, we consider the effect of its natal kick on the binary orbit. We use the prescription of Brandt & Podsiadlowski (1995) and the kick distribution of Hansen & Phinney (1997) to determine whether the binary remains bound or not. In the black hole case, we assume that the kick velocity is zero and estimate the remnant mass and ejected mass as in Eldridge & Tout (2004b).

If the system is unbound, we calculate the contribution of the secondary to the stellar lifetimes and SN type from our single-star models. The contribution from binaries that remain bound is taken from our secondary models. The initial mass taken for the secondary star is the initial secondary mass unless the star accreted material from the primary in which case we use the new mass after mass transfer.

Combining the model subsets creates our synthetic population of binary stars based on detailed models from which we can estimate the relative numbers of different stellar types and the relative rates of different types of SNe. We calculate these populations at five different metallicities, $Z = 0.001, 0.004, 0.008, 0.02$ and 0.04 .

2.2.7 Uncertainties

Uncertainties arise from assumptions we have made in the physical model for binary systems. The greatest uncertainty is that we do not model the primary and secondary in detail simultaneously. This means we are not able to model systems where q is close to 1. In these mass transfer can be quite efficient with the secondary accreting a large fraction of the mass of the primary (Cantiello et al. 2007). Our approximation is reasonable because for primaries with initial masses $\lesssim 60 M_{\odot}$, the secondary stars with $q \lesssim 0.9$ remain on the main sequence during the primary lifetime. The primaries $> 60 M_{\odot}$ with companions that evolve off the main sequence before the primary experiences an SN also rarely interact as both stars lose the hydrogen envelopes before becoming RSGs. The error introduced by this approximation is dwarfed by the uncertainty in our assumed initial parameter distribution for the binaries. If we only consider

binaries closer than $\log(a/R_{\odot}) < 3$, then we find that our RSG/WR ratio decreases by at least a factor of 2.

2.3 Defining stellar types

Stellar types may be defined by observable characteristics such as colour and luminosity. However, for a complete and accurate classification spectra are required. For example, some objects may initially appear to be BSGs but their spectra indicate that they are quite different and are in fact WR stars. WR spectra contain broad emission lines and weak or no hydrogen lines indicative of fast and dense stellar winds. In this work, we use the theoretical stellar definitions that are summarized in Table 1.

First, we only consider massive BSGs, RSGs and WR stars that have $\log(L/L_{\odot}) \geq 4.9$, equivalent to a luminosity cut-off of $M_{\text{bol}} \geq -7.5$. If we compare our models to single clusters with well-defined ages, the limit would not be critical. However, because we are considering a less-specific population with an assumed constant star formation rate, lowering the limit slightly to $\log(L/L_{\odot}) \geq 4.7$ does not significantly change our predicted BSG-to-RSG and RSG-to-WR ratios but does decrease the WC-to-WN ratio because a larger number of low-mass helium stars are included as WR stars.

BSGs and RSGs both have hydrogen envelopes but differ in their surface temperatures. BSGs are hot with $\log(T_{\text{eff}}/\text{K}) \geq 3.9$. This includes O, B and A stars. RSGs are cooler with $\log(T_{\text{eff}}/\text{K}) \leq 3.66$. This includes K and M stars. We show how these regions fit the tracks of our single-star evolution models in Fig. 1. RSGs are stars more massive than $12 M_{\odot}$ while BSGs are stars more massive than $20 M_{\odot}$. Our luminosity limit reduces contamination from AGB stars (Massey & Olsen 2003) in the RSG sample. The limit is also greater than the luminosity of stars that experience a blue loop during helium-burning. This feature is very sensitive to the details of convection included in the stellar models and so best excluded (Langer & Maeder 1995). Our models with blue loops lie outside our RSG definition so our predicted ratios are less sensitive to the complications introduced by the details of convection and mixing employed in our models.

We also consider the O supergiants (OSGs) which are a subset of the BSGs for the WR/O ratio. OSGs are the hottest hydrogen-rich stars with $\log(T_{\text{eff}}/\text{K}) \geq 4.48$ and a surface hydrogen mass fraction, $X > 0.4$. There is no luminosity limit for these stars as in Meynet & Maeder (2005).

The other stellar types we consider are WR stars. We define a WR star to be any star that has $\log(T_{\text{eff}}/\text{K}) \geq 4.0$ and a surface hydrogen mass fraction, $X < 0.4$. We also require that $\log(L/L_{\odot}) \geq 4.9$. Further to this, we subdivide WR stars into WNL, WNE and WC stars. In each case, the element nitrogen or carbon is dominant in their emission spectrum. The sequence is due to the exposure of nuclear burning products on the surface of the WR stars. We assume

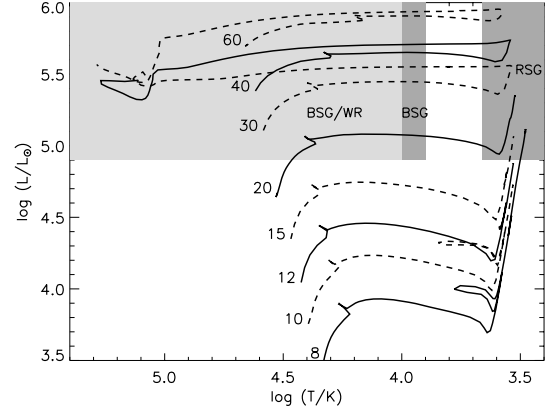


Figure 1. Hertzsprung–Russell diagram indicating regions that we include as BSGs, RSGs and WR stars with single-star tracks to indicate the mass ranges they sample. The numbers indicate the initial stellar mass in M_{\odot} for each track. The initial metallicity was $Z = 0.02$. The BSG and WR regions overlap in the lighter shaded region adjacent to the BSG region. The distinction between WR and BSG stars is made by surface hydrogen abundance.

that a WR star is initially a WNL star. When $X < 0.001$, it becomes a WNE star. The star becomes a WC star when $X < 0.001$ and $(x_C + x_O)/y > 0.03$, where x_C, x_O and y are the surface number fractions of carbon, oxygen and helium.

3 BLUE AND RED SUPERGIANT AND WOLF–RAYET LIFETIMES

In this section, we compare the stellar lifetimes of our single and primary models at two different metallicities. We calculate a mean lifetime from our primary models only to represent the effect on the lifetimes of RLOF and CEE. The mean lifetime for primary models with the same initial mass is calculated assuming a flat distribution in q and $\log a$.

The primary model BSG mean lifetimes are slightly increased relative to the single-star BSG lifetime. The total average lifetime for BSGs increases by 4–8 per cent and there is no trend with metallicity. This is because close merger systems extend the burning lifetimes of the primary star. Also stars initially too low in mass to be counted as BSGs accrete enough mass to rise above our luminosity limit.

The RSG lifetimes of our models are shown by the dotted lines in Figs 2 and 3. The single-star lifetimes at $Z = 0.004$ are longer than those at $Z = 0.02$. This is due to the reduction in mass-loss rates at the lower metallicity so more time is required for the hydrogen envelope to be removed. Our primary models have RSG lifetimes two to three times shorter. RLOF and CEE greatly reduce the number of RSGs by removing their hydrogen envelopes to form WR stars.

The WR lifetimes of our single stars are identical to those of Eldridge & Vink (2006). Mass loss affects the lifetimes. First, it determines the *total* WR lifespan by affecting the total stellar mass and thus the vigour of the nuclear reactions in the core. Secondly, stronger mass loss strips mass more quickly from the stellar surface, which leads to the exposure of hydrogen- and then helium-burning products and results in the appearance of different WR subtypes.

The WR lifetimes are longer at higher metallicities as the WR phase is entered at an earlier stage and there is a longer period of core helium burning during the WR phase because of larger pre-WR mass loss. The kink seen in the $Z = 0.02$ plot (Fig. 2) is due the fact that stars with masses below it undergo an RSG phase when mass is

Table 1. Our definitions of stellar types.

Name	$\log(T_{\text{eff}}/\text{K})$	$\log(L/L_{\odot})$	X	$\frac{(x_C + x_O)}{y}$
BSGs	≥ 3.9	≥ 4.9	> 0.4	–
RSGs	≤ 3.66	≥ 4.9	> 0.001	–
OSGs	≥ 4.48	–	> 0.4	–
WR star	≥ 4.0	≥ 4.9	≤ 0.4	–
WNL star	≥ 4.0	≥ 4.9	≤ 0.4	–
WNE star	≥ 4.0	≥ 4.9	≤ 0.001	≤ 0.03
WC star	≥ 4.0	≥ 4.9	≤ 0.001	> 0.03

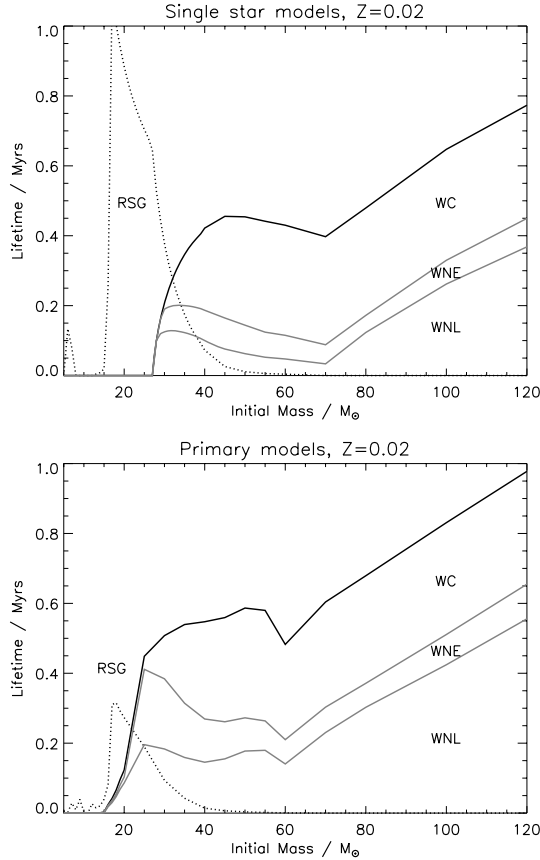


Figure 2. RSG, WNL, WNE and WC lifetimes at $Z = 0.02$. Upper panel: our single-star models. Lower panel: our primary models. The lifetimes of the binary stars are mean lifetimes assuming a flat q and $\log a$ distribution. Each region is labelled but progresses from the bottom to top panel by WNL, WNE and WC phases.

stripped and the surface hydrogen abundance drops below the limit set for WNL stars ($X_{\text{surface}} \leq 0.4$). However, the stars are still cool and sometime passes before they are hotter than the temperature limit (10^4 K). Stars more massive than the mass at the kink spend most of their evolution at temperatures hotter than this limit and become WR stars as soon as the surface abundance requirement is reached.

Our primary model WR lifetimes in Figs 2 and 3 have relatively minor differences as far as the total WR lifetimes are concerned. The main difference is that the minimum mass for a WR star is decreased to around $15 M_{\odot}$ at both metallicities. These stars will produce lower mass WR stars than are created by single stars.

The lifetimes of the WR subtypes at $Z = 0.02$ indicate that the primary models have longer WNE lifetimes than single stars and shorter WC lifetimes. The WR stars below the minimum mass limit for single WR stars do not have a WC phase and exist only as WN stars. At $Z = 0.004$, we see the same trend but many of the lower mass WR stars only have WNL phases.

4 RATIOS OF STELLAR NUMBER COUNTS

Counting and comparing the number of stars in different stellar populations is a useful method for investigating stellar evolution. A comparison between observed populations and those predicted by a stellar evolution code is only worthwhile if in the count stars are not

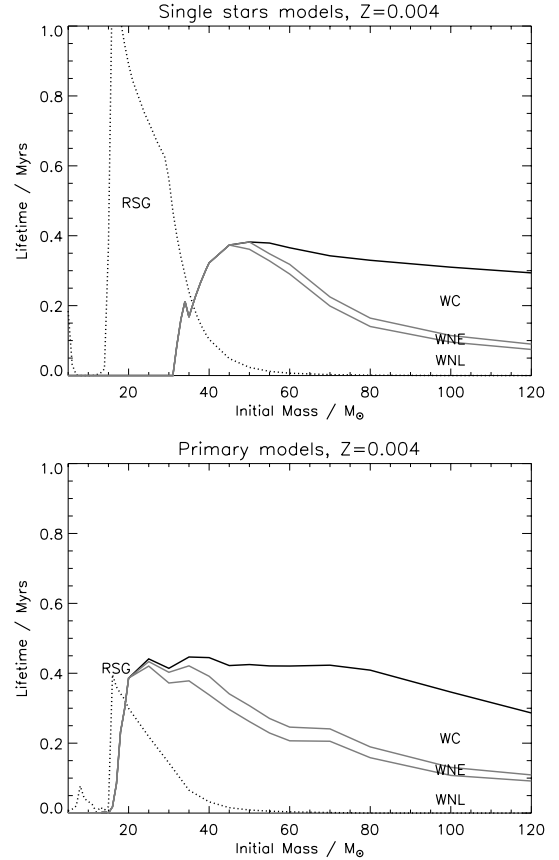


Figure 3. The same as for Fig. 2 but $Z = 0.004$.

missed or misclassified. Many older observations relied on groups of stars determined by photometry. The use of spectrometry has improved the accuracy and completeness of observational surveys (Massey & Olsen 2003).

The metallicity mass fraction of the observed stellar populations was calculated from the $\log [O/H] + 12$ values and comparing them to the values from our sets of models. Because this process is ambiguous and the position of solar metallicity for the mass-loss scaling is indistinct, we have assumed that the metallicities are uncertain by 25 per cent.

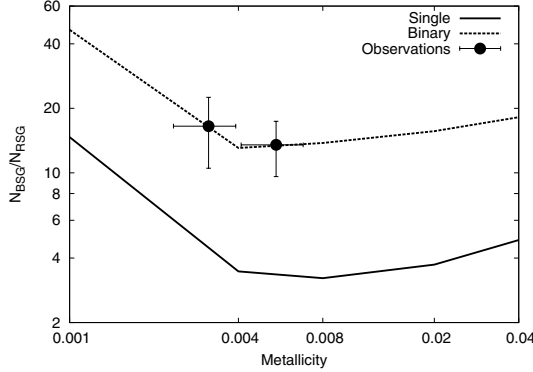
4.1 Blue-to-red supergiant ratio

The ratio of the number of BSGs to the number of RSGs has been a problem in stellar astrophysics for some time (Langer & Maeder 1995). Observations tend to indicate that the BSG/RSG ratio should decrease with metallicity while most stellar evolution codes predict a constant or increasing ratio. Eggenberger, Meynet & Maeder (2002) suggested that the situation could be improved by using spectroscopy to confirm the identity of supergiants. If we compare our models to their observed trend, we find good agreement at solar metallicity but no agreement at Small Magellanic Cloud (SMC) metallicity. However, Chiosi et al. (1995) indicate that the SMC cluster Eggenberger et al. (2002) observed has a spread of ages similar to the age of the cluster itself; therefore, the ratio they observe is not due to a single population of stars with the same age.

Massey & Olsen (2003) provide a detailed observational study of RSGs in the Magellanic Clouds with rigid definitions for BSGs and RSGs (see Table 1). They found from observing the entire SMC and

Table 2. Observed numbers and population ratios of BSGs and RSGs. Values are taken from Massey & Olsen (2003).

System	$\log [O/H] + 12$	N_{BSG}	N_{RSG}	N_{BSG}/N_{RSG}
SMC	8.13	1484	90	16 ± 6
LMC	8.37	3164	234	14 ± 4

**Figure 4.** Ratio of the numbers of BSGs to RSGs versus metallicity. Observations are taken from Massey & Olsen (2003). The solid line is from our single-star models, while the dashed line is from our binary models.

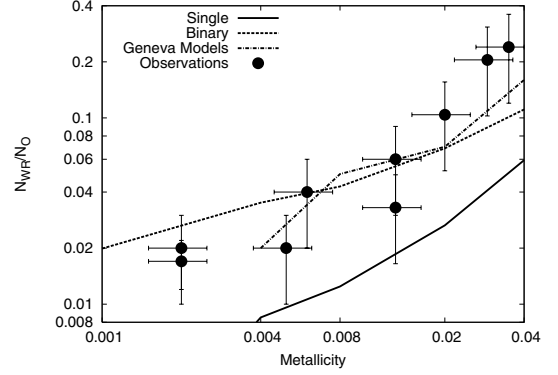
LMC that the ratios of BSGs to RSGs were 16 and 14, respectively (see Table 2).

Comparing the observations to predicted values from our models in Fig. 4 we find that single stars predict too low a value because there are either too many RSGs, too few BSGs or a combination of these two. Extra BSGs can be made via stellar mergers. Such stars are seen in globular clusters when the mass of the merged star is greater than the mass of the cluster turn-off; these are blue stragglers (Sills et al. 2000). The second binary effect is that stars below the minimum initial single-star mass for a WR star will lose their hydrogen envelopes to become WR stars because of RLOF or CEE. These are stars that would have been RSGs and therefore the total number is reduced. In combination, these processes increase the predicted BSG/RSG ratio as our binary models show.

The binary model ratio is dependent on how we choose the distribution of binaries in q and $\log(a/R_\odot)$. In our binary population, we include very wide binaries, $\log(a/R_\odot) \geq 3$, which evolve as single stars so our binary population is a mix of interacting binaries and single stars. Approximately, one-third of our primary models evolve as single stars. Therefore, to reproduce observations, two-thirds of all stars must be in interacting binaries. If our binary models are not completely correct, something extra, such as rotation, may decrease the required fraction of interacting binaries. Maeder & Meynet (2001) find that rotation has a strong effect on the BSG-to-RSG ratio but the trend they found was that the BSG-to-RSG ratio decreased rather than increased.

4.2 Wolf-Rayet-to-O supergiant ratio

The WR-to-OSG ratio has been studied for sometime (Maeder & Meynet 1994). If binaries leave the RSG population to become WR stars, then this ratio should increase if the BSG-to-RSG ratio decreases. The observed ratio is less certain than the BSG-to-RSG ratio because there is greater uncertainty in the completeness of

**Figure 5.** Ratio of the numbers of WR stars to OSGs versus metallicity. Observations are taken from Maeder & Meynet (1994). The solid line is our single-star models, while the dashed line is our binary models. The dash-dotted line for the Geneva models is taken from Meynet & Maeder (2005). The y-axis error bars are an assumed error of 50 per cent of the values given by Maeder & Meynet (1994).

the observations (Massey 2003). However, the trend that the ratio decreases with metallicity is well established (Crowther 2007).

Fig. 5 shows that our single-star models underpredict the ratio while our binary models are in better agreement, as are the Geneva rotating models. This is because in our models more stars are stripped off their envelopes and become WR stars. There is also a contribution to the OSG population from stellar mergers and secondary accretion as for the BSG/RSG ratio above. The trend our binary models predict with metallicity is a little too shallow but within the uncertainty of the observed ratios. This again could indicate that something extra may need to be included in our models.

4.3 RSG-to-Wolf-Rayet ratio

The RSG-to-WR ratio compares the relative populations of the two stellar types that have completed core hydrogen burning and so measures the influence of mass loss.

In Table 3, we list the observed populations. We plot the ratio in Fig. 6; it decreases dramatically with increasing metallicity. Such a change would require a stronger scaling of mass loss with metallicity than we presently employ.

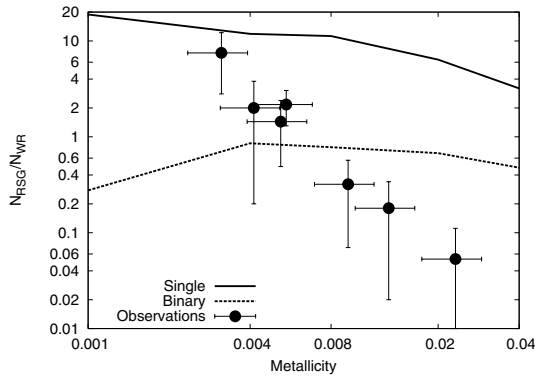
Our single-star models agree with the observations at SMC metallicity while our binary models agree with the observations around LMC metallicity. One way to match the observed trend between these metallicities is to have a metallicity-dependent binary fraction. However, something extra is still required around solar metallicity to get an exact agreement. At the higher metallicities, the ratios are based on a small number of observed stars (see Table 3) and therefore do not sample the full binary parameter space. Furthermore,

Table 3. Observed numbers and population ratios of RSG and WR stars. The values are taken from Massey (2003).

System	$\log [O/H] + 12$	N_{RSG}	N_{WR}	N_{RSG}/N_{WR}
SMC	8.13	90	12	7.5 ± 4.7
NGC6822	8.25	8	4	2.0 ± 1.8
M33(o)	8.35	26	18	1.44 ± 0.95
LMC	8.37	234	108	2.17 ± 0.87
M33(m)	8.6	7	22	0.32 ± 0.25
M33(i)	8.75	3	17	0.18 ± 0.16
M31	9	1	19	0.053 ± 0.058

Table 4. Observed numbers and population ratios of WC and WN stars. The values are taken from Meynet & Maeder (2005).

System	$\log [\text{O}/\text{H}] + 12$	N_{WC}	N_{WN}	$N_{\text{WC}}/N_{\text{WN}}$
SMC	8.13	1	11	0.083 ± 0.10
NGC6822	8.25	0	4	0.000 ± 0.20
M33(o)	8.35	3	16	0.190 ± 0.17
LMC	8.37	17	91	0.190 ± 0.11
M33(m)	8.6	12	35	0.370 ± 0.25
MW(<3 kpc)	8.7	30	35	0.880 ± 0.52
M33(i)	8.75	11	19	0.580 ± 0.42
M31	9	13	14	0.900 ± 0.66

**Figure 6.** Ratio of the number of RSG to WR stars versus metallicity. The observations are taken from Massey (2003). The solid line is from our single-star models, while the dashed line is from our binary models.

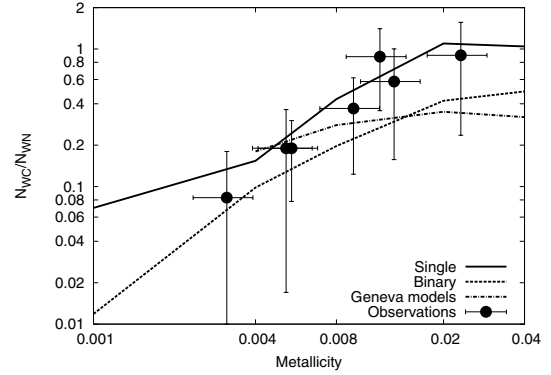
small numbers mean that our assumptions of constant star formation and IMF become invalid. For example, if all the WR stars are in very close binaries, the RSG/WR ratio would be even smaller than we estimate. A large number of stars must be observed to calculate the population ratio to ensure that the full range of possible binary systems is probed.

4.4 WC-to-WN ratio

Finally, we consider a ratio which provides a measure of the relative lifetimes of the two main WR star types: WN and WC (we include WO with WC). The lifetimes of the two types are determined by the mass-loss rates of WR stars.

We plot the observations and predicted ratios in Fig. 7; it shows our predicted ratios and the most-recent Geneva group rotating models (Meynet & Maeder 2005) for comparison. The trend of the observations is for the ratio to decrease with metallicity. In agreement with the results of Eldridge & Vink (2006), we find that the single-star models that scale the mass-loss rate of WR stars with initial metallicity agree with the observed trend.

The binary models in this case give a lower WC/WN ratio than the single-star models. This is because, as can be seen in Figs 2 and 3, the lifetimes of WN stars increase by a greater factor than the lifetimes of WC stars in binaries. If we combine a population of single and binary stars, the resulting ratio is too low and requires an increase in the WC population relative to the WN population to regain an improved agreement. The result is similar to that found by Vanbeveren et al. (2007).

**Figure 7.** Ratio of the number of WC to WN stars versus metallicity. The observations and the dash-dotted line for the Geneva models are taken from Meynet & Maeder (2005). The solid line is from our single-star models, while the dashed line is from our binary models.

5 SUPERNOVA PROGENITORS

There are many studies which investigate the connection between SNe and massive stars. Some studies consider single-star evolution and predict the initial parameter space and the relative rate of different SN types (Heger et al. 2003; Eldridge & Tout 2004b; Hirschi, Meynet & Maeder 2004), while other studies are concerned with the evolution of binary stars (Podsiadlowski et al. 1992; de Donder & Vanbeveren 2003; Izzard et al. 2004). In this section, we use our single- and binary-star models to predict the relative SN rates and determine how they vary with metallicity. First, we link our models to each SN type and then, secondly, we predict how the relative SN rates vary with metallicity.

Core-collapse SNe are classified according to their light curve shapes and spectra. Matching stellar models to observed SNe is difficult and example schemes can be found in Heger et al. (2003) and Eldridge & Tout (2004b). Here, we check the amount of hydrogen in the progenitor model: if there is more than $0.001 M_{\odot}$ of hydrogen left in the stellar envelope, then the SN is of Type II, otherwise Type Ib/c.

There are many subtypes of SNe. The main distinguishing criterion is the mass of the hydrogen or helium envelope at the time of explosion but sometimes the circumstellar environment must also be considered (Heger et al. 2003; Eldridge & Tout 2004b). In this paper, we group Type II SN subtypes (e.g. P, L) together as Type II and Type Ib SN and Type Ic SN subtypes together as Type Ib/c. In our single-star models, the initial mass range of Type Ib/c progenitors is restricted to the most-massive stars (Eldridge & Tout 2004b). In our binary-star models, the full range of masses can lead to Type Ib/c SNe.

SN rates in different galaxy types have been measured for some time (Cappellaro et al. 1997; Cappellaro, Evans & Turatto 1999) and, more recently, SN observations have been used to determine how the relative rate of Type Ib/c-to-Type II SNe varies with metallicity (Prantzos & Boissier 2003). The errors especially in the absolute rates of the searches are considerable owing to the small sample size and the uncertainties in the completeness. The relative rates are less uncertain as the selection effects are of similar magnitude and cancel.

We plot our predicted SN rate ratios against the observed ratios in Fig. 8. The observations indicate a general trend of a decreasing rate of Type Ib/c SNe relative to Type II SNe as metallicity decreases. This is as expected owing to the decreasing strength of

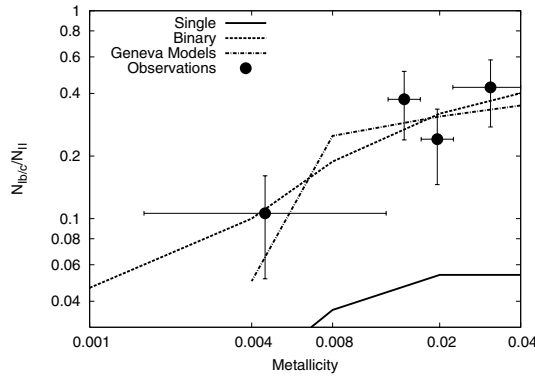


Figure 8. The observed and predicted ratios of the Type Ib/c SN rate to the Type II SN rate. Observations are taken from Prantzos & Boissier (2003). The Geneva model predictions are taken from Meynet & Maeder (2005). The upper line is for their rotating models, while the lower line is from their non-rotating models.

stellar winds with reduced metallicity meaning that fewer stars lose all the hydrogen before core-collapse.

We find that our theoretical predictions agree with the trend indicated by the observations. However, the single-star models predict a lower relative rate for Type Ib/c SNe than the observations and the binary-star models predict a value that agrees with the observations. We also plot the SN rate ratio predicted by the Geneva rotating models (Meynet & Maeder 2004) which agree with observations. The conclusion we draw is that we must consider rotating models and/or binary-star models to exactly simulate the observations.

6 DISCUSSION AND CONCLUSIONS

We have compared our stellar models of massive stars to several observations and find that by including binary stars we achieve better agreement. This is because duplicity increases the chance of a star losing its hydrogen envelope which leads to fewer RSGs, more WR stars and more Type Ib/c SNe than single-star models predict as required by observations.

Problems remain and the agreement is not perfect. The BSG/RSG ratio and RSG/WR ratio indicate that we still predict too many RSGs or not enough WR stars. Also the binary models predict too many WN stars and too few WC stars. Physics we have not included in our models might resolve these problems. The main culprit is rotation. It has two effects on our predictions. First, it introduces mixing that extends the time stars spend on the main sequence and therefore increases the number of BSGs. Secondly, if rotation is rapid it enhances mass loss by reducing the depth of the potential from which mass must escape and therefore increases the population of WR stars at the expense of the RSG population. Rotationally enhanced mass loss affects the WC/WN ratio by shortening the WN lifetimes. However, the effect of rotation can be much more complex than these simple effects. For example, Maeder & Meynet (2001) find that the BSG-to-RSG ratio is decreased rather than increased by rotation owing to a change in the internal helium gradient at the hydrogen-burning shell. In addition, tides in a binary may boost the importance of rotation during important phases of evolution and complicate the situation further (Petrovic et al. 2005a,b).

Another limitation of our models is that we do not include mass-losing eruptions that are common in the luminous-blue variable (LBV) stars. These most-massive stars experience giant outbursts, losing large amounts of mass in one short event. This has dramatic

implications for the evolution of the object (Smith & Owocki 2006). There is growing evidence that SN progenitors can experience these outbursts prior to the SN explosion (Kotak & Vink 2006; Pastorello et al. 2007). Such outbursts would have a similar effect on stellar populations to that of rotation. They reduce the time stars spend as RSGs and could reduce the time taken to remove the helium envelopes for WN stars. Therefore, a better understanding of these outbursts may also improve agreement between stellar models and observations.

In summary, binary stars must be considered when comparing stellar evolution models to observations. However, binary evolution alone cannot explain all the observations. Fine-tuning of stellar models is still required and the effect of enhanced mass loss owing to rotation or LBV-like eruptions must be further considered.

ACKNOWLEDGMENTS

The authors would like to thank the referee Andre Maeder for his helpful comments that improved this paper. JJE conducted part of this work during his time at the IAP in France as a CRNS post-doc. The remainder of this work was carried out as part of the award ‘Understanding the lives of massive stars from birth to supernovae’ made under the European Heads of Research Councils and European Science Foundation EURI Awards scheme and was supported by funds from the Participating Organisations of EURI and the EC Sixth Framework Programme. CAT thanks Churchill College, Cambridge, for his Fellowship. RGI thanks the NWO for his present fellowship in Utrecht. JJE also thanks Stephen Smartt, Norbert Langer and Onno Pols for useful discussion.

REFERENCES

- Belczynski K., Kalogera V., Bulik T., 2002, *ApJ*, 572, 407
- Brandt N., Podsiadlowski P., 1995, *MNRAS*, 274, 461
- Cameron A. G. W., Mock M., 1967, *Nat*, 215, 464
- Cantiello M., Yoon S.-C., Langer N., Livio M., 2007, *A&A*, 465, L29
- Cappellaro E., Turatto M., Tsvetkov D. Yu., Bartunov O. S., Pollas C., Evans R., Hamuy M., 1997, *A&A*, 322, 431
- Cappellaro E., Evans R., Turatto M., 1999, *A&A*, 351, 459
- Chiosi C., Vallenari A., Bressan A., Deng L., Ortolani S., 1995, *A&A*, 293, 710
- Crowther P. A., 2007, *ARA&A*, 45, 177
- Crowther P. A., Dessart L., Hillier D. J., Abbott J. B., Fullerton A. W., 2002, *A&A*, 392, 653
- de Donder E., Vanbeveren D., 2003, *New Astron.*, 8, 817
- de Donder E., Vanbeveren D., 2004, *New Astron.*, 48, 861
- de Jager C., Nieuwenhuijzen H., van der Hucht K. A., 1998, *A&AS*, 72, 259
- Deupree R. G., 2001, *ApJ*, 552, 268
- Dray L. M., Tout C. A., 2003, *MNRAS*, 341, 299
- Dray L. M., Tout C. A., 2007, *MNRAS*, 376, 61
- Eggleton P. P., 1971, *MNRAS*, 151, 351
- Eggleton P. P., 1983, *ApJ*, 268, 368
- Eldridge J. J., Tout C. A., 2004a, *MNRAS*, 348, 201
- Eldridge J. J., Tout C. A., 2004b, *MNRAS*, 353, 87
- Eldridge J. J., Vink J. S., 2006, *A&A*, 452, 295
- Eggenberger P., Meynet G., Maeder A., 2002, *A&A*, 386, 576
- Ferguson J. W., Alexander D. R., Allard F., Barman T., Bodnarik J. G., Hanschildt P. H., Heffner-Wong A., Tamanai A., 2005, *ApJ*, 623, 585
- Hansen B. M. S., Phinney E. S., 1997, *MNRAS*, 291, 569
- Heger A., Langer N., 2000, *ApJ*, 544, 1016
- Heger A., Langer N., Woosley S. E., 2000, *ApJ*, 528, 368
- Heger A., Fryer C. L., Woosley S. E., Langer N., Hartmann D. H., 2003, *ApJ*, 591, 288

- Heger A., Woosley S. E., Spruit H. C., 2005, *ApJ*, 626, 350
Hirschi R., Meynet G., Maeder A., 2004, *A&A*, 425, 649
Hurley J. R., Pols C. A., Tout O. R., 2000, *MNRAS*, 315, 543
Hurley J. R., Tout C. A., Pols O. R., 2002, *MNRAS*, 329, 897
Izzard R. G., Tout C. A., 2003, *PASA*, 20, 345
Izzard R. G., Ramirez-Ruiz E., Tout C. A., 2004, *MNRAS*, 348, 1215
Izzard R. G., Dray L. M., Karakas A. I., Lugaro M., Tout C. A., 2006, *A&A*, 460, 565
Kotak R., Vink J. S., 2006, *A&A*, 460, L5
Kroupa P., Tout C. A., Gilmore G., 1993, *MNRAS*, 262, 545
Kudritzki R. P., Pauldrach A., Puls J., 1987, *A&A*, 173, 293
Langer N., Maeder A., 1995, *A&A*, 295, 685
Livio M., Soker N., 1984, *MNRAS*, 208, 763
Maeder A., Meynet G., 1994, *A&A*, 287, 803
Maeder A., Meynet G., 2001, *A&A*, 373, 555
Massey P., 2003, *ARA&A*, 41, 15
Massey P., Olsen K. A. G., 2003, *AJ*, 126, 2867
Meynet G., Maeder A., 1997, *A&A*, 321, 465
Meynet G., Maeder A., 2003, *A&A*, 411, 543
Meynet G., Maeder A., 2004, *A&A*, 422, 225
Meynet G., Maeder A., 2005, *A&A*, 429, 581
Meynet G., Maeder A., 2007, *A&A*, 464L, 11
Nugis T., Lamers H. J. G. L. M., 2000, *A&A*, 360, 227
Paczynski B., 1976, in Eggleton P., Mitton S., Whelan J., eds, *Proc. IAU Symp. 73, Structure and Evolution of Close Binary Systems*. Reidel, Dordrecht, p. 75
Pastorello A. et al., 2007, *Nat*, 447, 827
Petrovic J., Langer N., Yoon S.-C., Heger A., 2005a, *A&A*, 435, 247
Petrovic J., Langer N., van der Hucht K. A., 2005b, *A&A*, 435, 1013
Podsiadlowski Ph., Joss P. C., Hsu J. J. L., 1992, *ApJ*, 391, 246
Podsiadlowski P., Langer N., Poelarends A. J. T. R. S., Heger A., Pfahl E., 2004, *ApJ*, 612, 1044
Podsiadlowski Ph., Morris T. S., Ivanova N., 2006, in Kraus M., Miroshnichenko A. S., eds, *ASP Conf. Ser. Vol. 355, Stars with the B [e] Phenomenon*. Astron. Soc. Pac., San Francisco, p. 259
Pols O. R., Tout C. A., Eggleton P. P., Han Z., 1995, *MNRAS*, 274, 964
Popov D. V., 1993, *ApJ*, 414, 712
Prantzos N., Boissier S., 2003, *A&A*, 406, 259
Sills A., Bailyn C. D., Edmonds P. D., Gilliland R. L., 2000, *ApJ*, 535, 298
Smartt S. J., Gilmore G. F., Tout C. A., Hodgkin S. T., 2002, *ApJ*, 565, 1089
Smartt S. J., Maund J. R., Hendry M. A., Tout C. A., Gilmore G. F., Mattila S., Benn C. R., 2004, *Sci*, 303, 499
Smith N., Owocki S. P., 2006, *ApJ*, 645, L45
Turatto M., Benetti S., Pastorello A., 2007, in Immler S., McCray R., eds, *AIP Conf. Ser. Vol. 937, Supernova 1987A: 20 years After*. Am. Inst. Phys., New York
Vanbeveren D., 2001, in Vanbeveren D., ed., *ASSL Vol. 264, The Influence of Binaries on Stellar Population Studies*. Kluwer Academic Publishers, Dordrecht, p. 249
Vanbeveren D., Van Bever J., Belkus H., 2007, *ApJ*, 662, L107
Van Dyk S. D., Li W., Filippenko A. V., 2003, *PASP*, 115, 1289
Vázquez G. A., Leitherer C., Schaerer D., Meynet G., Maeder A., 2007, *ApJ*, 663, 995
Vink J. S., de Koter A., 2005, *A&A*, 442, 587
Vink J. S., de Koter A., Lamers H. J. G. L. M., 2001, *A&A*, 369, 574
Wellstein S., Langer N., 1999, *A&A*, 350, 148
Woosley S. E., Heger A., Weaver T. A., 2002, *RvMP*, 74, 1015
Young T. R., Smith D., Johnson T. A., 2005, *ApJ*, 625, L87

This paper has been typeset from a \LaTeX file prepared by the author.